Remote Sensing of Environment 114 (2010) 1099–1107

Contents lists available at ScienceDirect

Remote Sensing of Environment

journal homepage: www.elsevier.com/locate/rse

Estimating average tree crown size using spatial information from Ikonos and QuickBird images: Across-sensor and across-site comparisons

Conghe Song [a,*], Matthew B. Dickinson [b], Lihong Su [a], Su Zhang [a], Daniel Yaussey [b]

[a] Department of Geography, CB# 3220, 205 Saunders Hall, University of North Carolina at Chapel Hill, Chapel Hill, NC 27599, USA
[b] US Forest Service, Northern Research Station, 359 Main Road, Delaware, OH 43015, USA

A R T I C L E I N F O

Article history:
Received 9 February 2009
Received in revised form 30 December 2009
Accepted 31 December 2009

Keywords:
Tree crown size
Image spatial information
Ikonos
QuickBird

A B S T R A C T

The forest canopy is the medium for energy, mass, and momentum exchanges between the forest ecosystem and the atmosphere. Tree crown size is a critical aspect of canopy structure that significantly influences these biophysical processes in the canopy. Tree crown size is also strongly related to other canopy structural parameters, such as tree height, diameter at breast height and biomass. But information about tree crown sizes is difficult to obtain and rarely available from traditional forest inventory. The study objective was to test the hypothesis that a model previously developed for estimation of tree crown size can be generalized across sensors and sites. Our study sites include the Racoon Ecological Management Area in southeast Ohio, USA and the Duke Forest in North Carolina Piedmont, USA. We sampled a series of circular plots in the summers of 2005 and 2007. We derived average tree crown diameter (CD) for trees with diameter at breast height (DBH) greater than 6.4 cm (2.5 in) for each sampling plot. We developed statistical models using image spatial information from Ikonos and QuickBird images as the independent variable and CD for stands in Ohio as the dependent variable. The models provide an explanation of tree crown size for the hardwood stands comparable to other approaches ($R^2 = \sim 0.5$ and RMSE = 0.83 m). Moreover, the models that estimate tree crown size using the ratio of image variances at two spatial resolutions can be applied across sensors and sites, i.e. the statistical models developed with Ikonos images can be applied directly to estimate tree crown size with QuickBird image, and the statistical models developed in Ohio can be applied directly to estimate tree crown size with images in North Carolina. These results indicate that the model developed based on image variance ratio at two spatial resolutions can be used to take advantage of existing sampling plot data and images to estimate CD with more recent images, enhancing the efficiency of forest resources inventory and monitoring.

© 2010 Elsevier Inc. All rights reserved.

1. Introduction

Forest canopy is the medium for energy, mass, and momentum exchanges between the forest ecosystem and the atmosphere. These exchanges determine the nature of goods and services that terrestrial ecosystems can offer and depend on canopy structure (Chen & Coughenour, 1994; Ni et al., 1997; Song et al., 2009). Tree crown size is one of the key canopy structural parameters because crowns are the space within which leaves are attached to the trees. Thus, for a stand with given leaf area index (LAI), crown size indicates how the leaves are organized in space. Associating leaves with crowns allows the representation of gaps between crowns, making simulation of sub-canopy solar radiation regimes more realistic (Song & Band, 2004). Gaps in the canopy are critical for modeling plant regeneration on the forest floor (Botkin et al., 1972; Shugart & West, 1977; Urban, 1990). Consideration of between-crown gaps is a major step toward more realistic characterizations of forest canopies from the traditional turbid medium representation where leaves are assumed to be randomly distributed in the entire canopy space without crown boundaries. Song et al. (2009) found that a uniform canopy representation can lead to overestimation of radiation interception, transpiration, and carbon assimilation in the canopy. Therefore, tree crown size is essential for more accurate understanding of ecosystem function. Unlike diameter at breast height (DBH), tree crown size is difficult to measure in the field. The ability to estimate tree crown size from remote sensing would provide a major benefit for research and management efforts.

Earlier remotely sensed data from space are not suitable for tree crown size retrieval because the pixel size is usually much bigger than a typical tree crown size. Strahler et al. (1986) referred to the spatial resolution of these images with respect to object size as L-resolution. Previous efforts to estimate tree crown size from Landsat TM imagery achieved some success (Cohen & Spies, 1992; Franklin & Strahler, 1988; Woodcock et al., 1994, 1997; Wu & Strahler, 1993). Due to the limitation in spatial resolution of remote sensing data from space earlier, a significant amount of work extracting tree crown size was based on high spatial resolution air photos (Brandtberg & Walter,

* Corresponding author. Tel.: +1 919 843 4764; fax: +1 919 962 1537.
E-mail address: csong@email.unc.edu (C. Song).

0034-4257/$ – see front matter © 2010 Elsevier Inc. All rights reserved.
doi:10.1016/j.rse.2009.12.022

1998; Culvenor, 2002; Leckie et al., 2003; Pollock, 1996; Wulder et al., 2000). Automatic detection of tree crowns from aerial photos is generally accomplished in two steps: (1) tree crown detection and (2) tree crown delineation (Pouliot et al., 2002). Automatic detection requires that the pixel size be much smaller than the tree crown size to define tree crown boundaries; however, high spatial resolution increases variation in within-crown brightness, making tree crown identification difficult. Automatic detection often assumes that each tree has a distinct boundary with no overlap between adjacent crowns, but such overlap is common in a real forest. Therefore, validation shows that direct delineation of tree crowns on high spatial resolution aerial photos can lead to significant errors in both the number of crowns and the crown size on a tree-by-tree basis (Brandtberg & Walter, 1998; Leckie et al., 2003; Wulder et al., 2000). The detection–delineation approach can achieve much better accuracy in tree crown diameter when aggregated among multiple plots (Pouliot et al., 2002). Brown et al. (2005) evaluated the potential of very high spatial resolution aerial photos in estimating biomass with manual delineation of individual crowns and found that working with the aerial photos took only a third of the time needed for conventional fieldwork.

Small footprint Lidar data offer an alternative promising approach to estimate tree crown size remotely (Falkowski et al., 2006, 2008; Lee & Lucas, 2007; Persson et al., 2002; Popescu & Wynne, 2004; Popescu et al., 2003). Similar to optical imagery, extraction of tree crown size with Lidar data also requires two steps: (1) tree detection, and (2) tree crown delineation. The techniques used for tree detection in optical imagery are also been widely used with Lidar data, particularly the local maximum approach. Lidar imagery directly provides height information for the top of the canopy. Extracting tree crown size using Lidar data relies on the canopy height model (CHM), which is derived from subtracting the digital elevation model for the ground from Lidar height data (Popescu et al., 2003).

Although small footprint Lidar data have advantage over high spatial resolution optical imagery with canopy height information, the data are extremely expensive to acquire at present. High spatial resolution optical images, such as Ikonos and QuickBird, are much cost effective, and they are now available for almost anywhere in the world. Asner et al. (2002) studied the potential of using Ikonos imagery to map tree crown size by comparing measurements on the image with crown size measured on the ground, and they found that measurements on the image were biased toward large trees. Clark et al. (2004) demonstrated the value of Ikonos image in forest demographic research. Palace et al. (2008) developed an automatic tree crown detection and delineation algorithm, and found that it provided better estimates of mean crown width than manual delineation from Asner et al. (2002). However, Palace et al. (2008) found that the automatic algorithm was not able to detect understory trees and overestimated the size and frequency of large trees. Wulder et al. (2004) compared an Ikonos image with an airborne image collected at the same spatial resolution and found that the 1 m panchromatic Ikonos image can be used to identify 85% of tree crowns, but with a 51% commission error. Song and Woodcock (2003) developed a new approach to extract tree crown size based on the behavior of image semivariograms at different spatial resolutions to estimate average tree crown size on a stand basis. The approach performed well for stands dominated by conifer trees, but not as well for hardwood dominated stands (Song, 2007). Wolter et al. (2009) further advanced the approach of using image variance ratios by incorporating numerous other image spatial and spectral statistics to extract multiple canopy structure parameters, including tree crown size, based on SPOT images at 5 and 10 m spatial resolutions.

The objective of this paper is to further investigate the applicability of the Song-Woodcock (2003) model to hardwood dominated stands. We also intend to test the hypothesis that the approach has the potential to work across sensors and sites because the spatial information used in the algorithm depends only on the scene structure, not on the absolute brightness values. If validated, the model would provide a sound theoretical basis for mapping recent forest canopy structure using historical high resolution images and existing forest inventory plot data collected at the same time.

2. Theory

Each pixel in a remotely sensed image is tied to a location in space, thus, the brightness value of a pixel can be treated as a realization of a regionalized variable at the pixel location. Thus, the semivariogram tool in geostatistics can be used to understand the relationship between scene structure and the characteristics of the semivariogram. A semivariogram is a plot of semivariance against the lag that separates the points used to estimate the semivariance. Semivariance is defined as

$$\gamma_f(h) = \frac{1}{2}E\{(f(x)-f(x+h))^2\}, \tag{1}$$

where $\gamma_f(h)$ is the semivariance for points with a lag h in space; $f(x)$ is the realization of a spatial random function $f(.)$ at location x, and $f(x+h)$ is the realization of the same function at another point with a lag h from x. $E\{.\}$ denotes expectation.

Jupp et al. (1988) and Woodcock et al. (1988a) provided the theoretical basis for the linkage between the scene structure and the semivariogram derived from a remotely sensed image. Using high spatial resolution aerial photos, Woodcock et al. (1988b) showed that the range of the image semivariogram contains information on object size and the sill of the image semivariogram is related to the cover of objects. Remotely sensed images are always obtained with a finite size of instantaneous field of view (IFOV). The brightness value of a pixel in an optical imagery is determined by the spatial average of the reflected energy at a particular spectral range within the IFOV. Therefore, the spatial information of a remotely sensed imagery depends on both the scene structure and the size of the IFOV. For remotely sensed imagery over a relatively uniform and large forest, the range of the semivariogram for the image is the combined length of the object size and pixel size. Therefore, the range reflects the object size when the pixel size is significantly smaller than the object size. As the pixel size increases, the range is increasingly dominated by the pixel size, making extracting crown size difficult. In the meantime, the sill of the semivariogram also decreases as the pixel size increases. Jupp (1999) demonstrated the behavior of the semivariogram as a function of object size and the size of IFOV with a disc scene model. The model assumes an unbounded scene with discs in contrasting brightness or color randomly distributed in the scene. The discs can overlap, but the color of the disc remains the same in the overlapped area. The disc scene model is analogous to a forest scene when viewed from a space-borne satellite because the tree crowns in a two-dimensional image resemble discs. Based on the disc scene model, Song and Woodcock (2003) developed a model that relates the ratio of the sill at two spatial resolutions to the diameter of the object as

$$\frac{C_{Z1}}{C_{Z2}} = \frac{\int_0^1 tT(t)(e^{\lambda A_c T(tD_{p1}/D_o}-1)dt}{\int_0^1 tT(t)(e^{\lambda A_c T(tD_{p2}/D_o}-1)dt}, \tag{2}$$

where D_{p1} and D_{p2} are the diameters of IFOV at two spatial resolutions, and D_o is the diameter of the object (the discs); C_{Z1} and C_{Z2} are the sills of the regularized semivariograms at the spatial resolutions of D_{p1} and D_{p2}, respectively. We use r_{Z1Z2} to denote the ratio in the rest of the paper (e.g., r12 denotes the ratio of image variances at 1×1 m to that at 2×2 m). The disc area is A. $T(t)$ is the overlap function for the discs in the scene:

$$T(s) = \begin{cases} 1 & s=0 \\ \frac{1}{\pi}(t-\sin(t)) & s<1 \\ 0 & s\geq 1 \end{cases}, \tag{3}$$

where the quantity t is defined in $\cos(t/2) = s$, and s is the standardized distance for D_o with respect to the lag (h), i.e. $s = h/D_o$. The variance ratio in Eq. (2) is independent of the brightness values of the pixels and depends on the scene structure only. Therefore, we can hypothesize that the ratio of image variances can be used to estimate tree crown size across sensors and/or sites.

For across-site and sensor's generalization, we used the models developed in Ohio and directly applied them to estimate tree crown size in North Carolina. The errors of the tree crown size estimation are measured with the root mean squared error (RMSE) between the estimated tree crown size and an independently measured set of tree crown size on the ground, i.e.

$$RMSE = \sqrt{\frac{\sum_{i=1}^{N} (\hat{D}_i - D_i)^2}{N}}, \tag{4}$$

where $\hat{D}_i$ and D_i are the estimated and the ground measured average crown diameters, respectively. It is important to note that the ground measured tree crown sizes were not used in model development.

3. Methodologies

3.1. Study sites

Two study sites were used in this study (Fig. 1). The first study site (39°11′59″ N, 82°23′46″ W) is located on the unglaciated Alleghany Plateau in southeast Ohio, USA. The study area included the 6430 ha Racoon Ecological Management Area (REMA) and the imbedded 194 ha Vinton Furnace Experimental Forest (VFEF) in Vinton County, OH. The REMA and VFEF are owned by the Forestland Group and are under active management. Ongoing research on the VFEF is jointly managed by the U.S. Forest Service, Northern Research Station, and the Forestland Group. The area is dominated by mixed oak–maple forests. The second study site (35°58′41″ N, 79°5′39″ W) is located in the Piedmont Plateau of North Carolina in the vicinity of the Blackwood Division of Duke Forest. Stands in the Duke Forest area include pure hardwoods and pines as well as varying degrees of mixture of the two. The second site is primarily used for testing the feasibility of across-site generalization.

3.2. Remotely sensed imagery

To test our hypothesis that the model using image variance ratios to predict tree crown size can be generalized across satellite sensors, two high spatial resolution images from two sensors were used. The first image was collected by the Ikonos satellite over REMA on June 14, 2006, with the sun zenith angle at 20.1° and the sensor viewing zenith angle at 8.2°. The nominal ground resolution was 0.83 m cross scan and 0.84 m along scan for the panchromatic band. The image was resampled to1×1 m spatial resolution at delivery. The second image was collected by the QuickBird satellite exactly over the same area on June 1, 2007, with the sun zenith angle at 18.8° and the sensor viewing zenith angle at 12.7°. The nominal ground resolution is 0.76 m cross scan and 0.79 m along scan for the panchromatic band. The image was resampled to 0.73×0.73 m at delivery. We further resampled the QuickBird image to 1×1 m spatial resolution to match that of the Ikonos image. We also generated a series of coarser spatial resolution images with pixel size in 2×2, 3×3, …, and 7×7 m with simple averaging for both images. Although both images were georectified before delivery, the two images do not overlay well. Because the geographic coordinates of the latter corresponded well to the GPS reading taken during the 2007 field

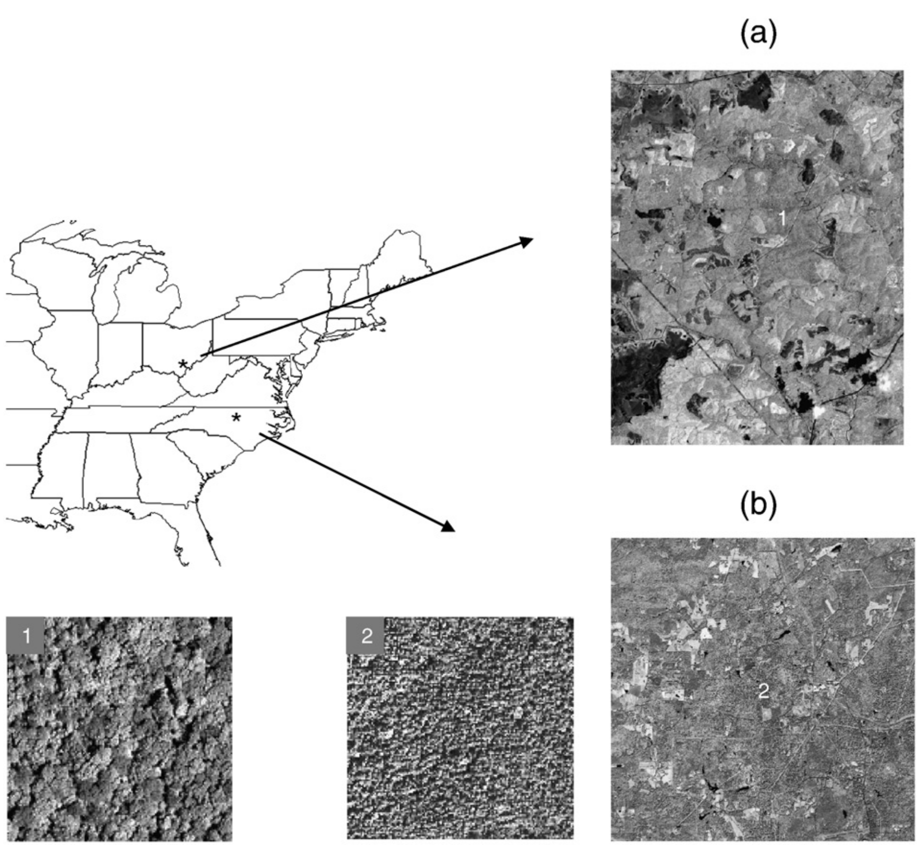

Fig. 1. Study sites: (a) Snap shot of the whole Ikonos image for the study site in Ohio. The size of the area is 9.2×11.8 km. (b) Snap shot of the whole Ikonos image for the study site in North Carolina. The size of the area is 10.0×10.0 km. The areas zoomed in (150×150 m) are for a hardwood stand in Ohio and a loblolly pine stand in North Carolina whose locations are marked in the image snap shots.

campaign, we registered the Ikonos image to the QuickBird image with 20 ground control points well distributed within the image with RMSE less than 1 pixel. We overlaid the two images and did not notice obvious mismatch in the image. Both images were relatively clear with cloud cover well under 20%. We did not perform any atmospheric correction for the images because the theory in Eq. (2) indicates that atmospheric correction would not have a significant effect on the image variance ratio (Song & Woodcock, 2003).

Although the two images were acquired with the same radiometric resolution (11 bits) on exactly the same place and near the same day of the year, the panchromatic Ikonos image was found to have a significantly higher mean ($M_{ik}=546.2$) and standard deviation ($S_{ik}=129.9$) for the digital values than the mean ($M_{qb}=382.9$) and standard deviation ($S_{qb}=73.9$) for those from the QuickBird image after both images were resampled at 1×1 m spatial resolution. Wang et al. (2004) found similar differences in the images from the two sensors. Despite some management actions taken within VFEF for some stands during the year, these actions could not cause such big differences in the statistics for the whole scene. Therefore, the discrepancies were primarily caused by sensor differences, and these two images are well suited to test the hypothesis across sensor generalization.

A third image was collected on September 23, 2004 for the Blackwood Division of Duke Forest in North Carolina. The sun and sensor zenith angles were 38.0° and 6.7°, respectively. The cloud cover in the image is zero. This image was used to test the hypothesis of across-site generalization.

3.3. Fieldwork

The primary task of fieldwork is to collect tree crown size for sampling plots for model development. We conducted two fieldwork campaigns in the summers of 2005 and 2007, covering both REMA and Duke Forest. We located sampling plots in relatively uniform and large stands. The sampling plots are circular with a diameter at 30 m in general. But the plot size could range from 50 m in diameter in old-growth stands to 12 m in diameter in young stands because there are fewer large trees in an old-growth stand and many smaller trees in a young stand. The size of the plot is determined in the field based on the sampling experience. The goal of the sampling is to collect sufficient number of individuals such that a representative tree crown size can be derived from the samples. Once a plot boundary was marked, we measured the diameter at breast height (DBH) for each tree larger than 6.4 cm (2.5 in). The crown diameters (CD) were measured in two orthogonal directions with one measurement along the crown maximum. The mean of the two measurements was taken as the tree CD. Because it is extremely difficult and time consuming to measure tree crown size, it was impossible to directly measure CD for each tree in every plot. We took a sample of trees that spanned the diameter classes and species in each plot. At the end of the fieldwork, we pooled the DBH and CD by species and developed a species-specific allometry between DBH and CD for each site as

$$\ln(D_c) = b_0 + b_1 \ln(D_s), \tag{5}$$

where b_0 and b_1 are empirical parameters, and D_c and D_s are CD and DBH, respectively. With the allometry between CD and DBH, we applied the relationship to each other individual based on the DBH measured and its species, and an area based average CD was derived for each stand.

4. Results

4.1. Tree crown diameter and DBH

We measured 396 trees for canopy diameters for REMA and 238 trees for canopy diameters for Duke Forest in summer 2005. We developed the allometric relationship for each species based on Eq. (5). Table 1 shows the empirical parameters for the allometry for each species as well as the ensemble relationship after pooling all trees at each site. The relationship in Table 1 is statistically significant for each species. There are notable differences in the allometric relationships for the common species between the two sites. The ensemble relationship remains strong although with a somewhat lower R^2. We did not measure CD in the field in summer 2007 assuming the allometry we developed in 2005 be applicable in 2007 on a site-specific basis. We assume that the growth of CD from 2005 to 2007 at REMA is within the margin of measurement error. Therefore, these plots can be treated as a single dataset for model development with either the Ikonos or the QuickBird image. The average tree crown diameter for all plots, along with other canopy structure statistics, is given in Table 2 for both sites.

4.2. Tree crown diameter and image spatial information

Results between tree crown diameter and image spatial information for Duke Forest can be seen in Song (2007). The sampled plots at REMA naturally break into two groups: plots collected in 2005 (P05) and plots collected in 2007 (P07). We did a series of regression analyses between the ratio of image variances and the average plot CD for each of the images: Ikonos image collected in 2006 (I06) and QuickBird image collected in 2007 (Q07). The R^2 of these regression analyses are given in Table 3. The plots collected in 2005 have higher R^2 values for both I06 and Q07 than the plots collected in 2007. We created two dummy variables for the R^2 values in Table 3: one for the images and the other for the plots. Regression analysis for the dummy variables indicates that there is no significant difference between images (I06 vs.Q07), but there is a significant difference between plots (P05 vs. P07) in estimating CD. The highest R^2 for the 2005 plots is much higher than that for the hardwood stands in the study by Song (2007) but still lower than that for the coniferous stands. For the P05 and I06 combination, the highest R^2 (0.59) occurred for the ratio of variance at 2×2 m to that of 6×6 m spatial resolution with RMSE = 0.83 m, and for the P05 and Q07 combination the highest R^2 (0.60) took place for the ratio of variance at 2×2 m to that at

Table 1
Allometry between tree crown diameter (CD) and tree diameter at breast height (DBH): $\ln(\mathrm{CD}) = b_0 + b_1\ln(\mathrm{DBH})$. The relationships were developed based on field data collected in summer of 2005: (a) Allometry for species in REMA, OH, and (b) allometry for species in Duke Forest, NC.

Species	b_0	b_1	R^2	n
(a)				
Aspen	−0.6583	0.9710	0.66	26
Black cherry	0.1939	0.6829	0.70	12
Black gum	−0.8050	1.2456	0.71	6
Chestnut oak	0.1849	0.6708	0.70	39
Hickory	0.0207	0.7771	0.79	19
Red maple	0.5672	0.6042	0.55	55
Red oak	0.0124	0.776	0.74	32
Tulip poplar	−0.0542	0.7532	0.77	52
White oak	0.1040	0.7346	0.59	67
White pine	−0.3500	0.8710	0.79	66
All	0.0745	0.7213	0.63	396
(b)				
Loblolly pine	−1.1013	1.0201	0.77	103
Shortleaf pine	−0.5554	0.9123	0.82	15
Hickory	0.0707	0.8617	0.81	7
Red maple	0.2572	0.7841	0.74	20
Sweet gum	0.0661	0.7168	0.55	28
Tulip poplar	0.1720	0.6296	0.83	29
Red oak	0.2335	0.7056	0.56	8
White oak	−0.0438	0.8185	0.81	15
Others	0.4882	0.6028	0.58	13
All	−0.0435	0.6798	0.50	238

Table 2
Canopy structure for the sampled plots collected in the summers of 2005 and 2007: (a) plots in REMA, OH and (b) plots in Duke Forest, NC.

Plot ID	Time sampled	Plot diameter (m)	Mean DBH (cm)	Stem density (trees/ha)	Mean CD (m)
(a)					
1	June 2005	30	14.32	1599	3.47
2	June 2005	30	17.12	1320	4.21
3	June 2005	30	28.27	552	6.13
4	June 2005	30	33.19	481	7.53
5	June 2005	30	14.45	1344	3.81
6	June 2005	30	21.36	608	5.22
7	June 2005	30	21.25	608	5.64
8	June 2005	30	22.77	778	5.88
9	June 2005	30	31.47	410	7.05
10	June 2005	30	26.05	651	6.05
11	June 2005	30	22.86	608	5.63
12	June 2005	50	37.94	422	7.48
13	June 2005	50	36.47	275	7.62
14	June 2005	50	34.19	250	7.46
15	June 2005	30	22.57	863	5.04
16	June 2005	30	19.41	1089	4.58
17	June 2005	50	31.71	372	6.56
18	June 2005	30	22.12	665	5.24
19	June 2007	50	15.62	1471	4.43
20	June 2007	30	25.39	545	5.89
21	June 2007	30	13.7	1514	3.52
22	June 2007	40	25.19	613	5.73
23	June 2007	30	15.8	1287	4.20
24	June 2007	40	26.34	525	6.01
25	June 2007	30	13.08	1556	3.70
26	June 2007	30	13.94	1457	4.18
27	June 2007	12	17.84	1094	4.43
28	June 2007	30	16.81	1202	4.76
29	June 2007	30	25.19	707	5.91
30	June 2007	30	19.29	792	4.73
31	June 2007	30	13.68	1485	3.77
32	June 2007	30	30.73	453	6.57
33	June 2007	30	11.30	2051	3.29
34	June 2007	40	29.02	470	6.16
35	June 2007	30	17.33	1259	4.37
36	June 2007	30	25.01	651	5.51
37	June 2007	40	24.12	533	5.25
38	June 2007	30	24.6	396	5.10
39	June 2007	30	21.18	608	5.26
40	June 2007	40	26.59	501	6.00
(b)					
1	June 2005	30	17.56	1995	3.21
2	June 2005	30	25.78	806	4.86
3	June 2005	30	16.93	2080	2.92
4	June 2005	30	18.22	1811	2.99
5	June 2005	30	28.50	566	6.33
6	June 2005	30	19.90	1500	2.94
7	June 2005	30	18.59	1712	3.22
8	June 2005	30	24.96	608	5.99
9	June 2005	30	9.82	3240	3.13
10	June 2005	30	23.46	905	5.41
11	June 2005	15	6.04	8715	1.83
12	June 2005	40	21.24	668	4.98
13	June 2005	30	23.95	920	5.01
14	June 2005	40	28.61	613	5.01
15	June 2005	20	15.42	1974	2.88
16	June 2005	30	23.35	1160	4.61
17	June 2005	30	22.73	1075	4.38
18	June 2005	30	19.21	1174	5.35
19	June 2005	30	26.69	495	5.50
20	June 2005	30	21.37	1146	4.06
21	June 2005	30	20.57	1203	3.41

5×5 m spatial resolution with RMSE = 0.82 m. For the conifer stands studied by Song (2007), the highest R^2 (0.73) occurred for the ratio of variance at 2×2 m to that at 3×3 m spatial resolution with RMSE = 0.10 m. The better fit was primarily caused by the difference in canopy structure between the coniferous stands and the hardwood stands. Trees in a mature hardwood stand are bigger, and the canopy appears more continuous in a hardwood stand than in a coniferous stand. Similar difference between hardwoods and conifers were reported in other studies extracting tree crown size (Heurich, 2008; Popescu et al., 2003). Therefore, a bigger difference in the spatial resolution is needed for the ratio of image variances to best extract tree crown size for the hardwood stands.

Table 3
R^2 values for regression analyses between tree crown size and image variance ratio (r12 is the ratio of image variance around the sample plots at 1×1 m spatial resolution to that at 2×2 m spatial resolution). There are two sets of sampled plots: one collected in summer 2005 (P05) and the other collected in summer 2007 (P07). There are two images available: the Ikonos image acquired in summer 2006 (I06) and the QuickBird image acquired in summer 2007 (Q07). The asterisk indicates the maximum R^2 within the column.

Variance ratio	P05I06	P05Q07	P07I06	P07Q07
r12	0.400	0.461	0.362	0.331
r13	0.508	0.506	0.286	0.362
r14	0.540	0.544	0.398	0.364
r15	0.530	0.598	0.406	0.368
r16	0.566	0.576	0.401	0.387*
r17	0.576	0.47	0.427	0.336
r23	0.574	0.507	0.143	0.333
r24	0.588	0.563	0.354	0.348
r25	0.515	0.601*	0.387	0.362
r26	0.594*	0.573	0.384	0.387*
r27	0.575	0.436	0.395	0.322
r34	0.446	0.564	0.313	0.11
r35	0.277	0.555	0.385	0.244
r36	0.421	0.551	0.408	0.346
r37	0.482	0.354	0.428*	0.231

We combined P05 and P07 to test the hypothesis that the ratio of image variances at two spatial resolutions can be used to extract tree crown size across sensors and sites. Although P07 was not as good as P05 in extracting tree crown size, combining P05 and P07 more than doubles the sample size and provides greater confidence in the statistical results. Table 4 presents the regression analysis results between tree crown size and image spatial information with the combined plots for I06 and Q07, respectively. As expected, R^2 is lower for the combined plots than using P05 alone due to the effect of P07. It is obvious that the ratio of image variance between two spatial resolutions can be used to predict CD much better than the image variance at a single spatial resolution. We also analyzed the slope and intercept in Table 4 for the variance ratios that have a significant relationship with CD in Table 4 (shaded portion of the table). Fig. 1 shows that both the slope and intercept for the relationships between CD and variance ratio appear very close along the 1:1 line for I06 and Q07 images. We also notice a trend in the data scattering in Fig. 1. When R^2 between CD and the variance ratio is higher, the slope and intercept from I06 and Q07 are closer to the 1:1 line. Therefore, even though the Ikonos and QuickBird images have very different brightness values, the relationship between CD and the ratio of image variances converge from the two sensors.

Song (2007) was the first study that tested the theory of using the image variance ratio at two spatial resolutions (Song & Woodcock, 2003) to extract tree crown size with plot data measured in the field. The plots were dominated by coniferous trees. Although these plots are not ideal for cross-site application of variance ratio relationships with CD, we explored the feasibility by taking the relationship derived from the Ohio images and applying it to the North Carolina image. Based on Song (2007), the best image variance ratio to predict CD is r23 for the stands in North Carolina. The best variance ratio to predict CD is r26 for the Ikonos image and r25 for the QuickBird image for the hardwoods stand. We cannot use the best relationships in both sites for cross-site and image application due to the difference in forest types. We used the relationship between CD and r23 in Table 4 in this study from the Ikonos and QuickBird images and the image variance ratios produced from the Ikonos image in North Carolina to estimate

Table 4
Regression results for $Y = a + bX$, where X is a textural measurement, and Y is CD for the combined sampling plots. There is no data normalization between the Ikonos and QuickBird images. Note v1 is the image variance at 1×1 m spatial resolution, and so on, and r12 is the ratio of image variance at 1×1 m to that at 2×2 m, and so on. The shaded portion of the table includes the regression results with $P<0.0001$ for regressions between CD and variance ratios.

X	Ikonos				QuickBird			
	a	b	R^2	P	a	b	R^2	P
v1	2.3544	0.0004	0.2569	0.0007	2.7680	0.0012	0.2866	0.0004
v2	3.2974	0.0004	0.2824	0.0004	3.2226	0.0014	0.3266	0.0001
v3	3.6932	0.0005	0.2910	0.0003	3.5348	0.0015	0.3369	<.0001
v4	3.8008	0.0006	0.3063	0.0002	3.6603	0.0017	0.3616	<.0001
v5	3.9073	0.0007	0.3149	0.0001	3.7439	0.0020	0.3758	<.0001
v6	3.8889	0.0008	0.3342	<.0001	3.8173	0.0023	0.3996	<.0001
v7	4.0336	0.0009	0.3198	0.0001	3.9850	0.0024	0.3447	<.0001
r12	12.6713	−4.3422	0.4360	<.0001	14.3515	−6.5285	0.4617	<.0001
r13	9.4810	−1.6827	0.4351	<.0001	9.6689	−2.3709	0.4356	<.0001
r14	8.8420	−1.0846	0.4938	<.0001	8.7740	−1.4505	0.4648	<.0001
r15	8.0138	−0.6496	0.4640	<.0001	8.0992	−0.9242	0.4643	<.0001
r16	8.0606	−0.5318	0.4759	<.0001	7.6827	−0.6412	0.4740	<.0001
r17	7.8658	−0.4049	0.5040	<.0001	7.4093	−0.4598	0.4054	<.0001
r23	13.4876	−5.6324	0.3657	<.0001	13.5364	−6.2399	0.3802	<.0001
r24	11.6169	−3.3231	0.4939	<.0001	11.0470	−3.3664	0.4608	<.0001
r25	9.5384	−1.7540	0.4617	<.0001	9.5367	−1.9714	0.4726	<.0001
r26	9.6613	−1.4523	0.4861	<.0001	8.6576	−1.2585	0.4842	<.0001
r27	8.9997	−1.0115	0.5019	<.0001	8.1637	−0.8847	0.3943	<.0001
r34	15.4937	−7.7844	0.3383	<.0001	14.1120	−6.8202	0.2992	0.0001
r35	10.9490	−3.4051	0.3632	<.0001	12.0304	−4.1578	0.4283	<.0001
r36	11.6125	−3.0647	0.4204	<.0001	10.5828	−2.6848	0.5031	<.0001
r37	10.5826	−2.1144	0.4782	<.0001	9.1738	−1.5968	0.3434	<.0001
r45	11.6043	−4.9591	0.1874	0.0047	14.5025	−7.3381	0.2731	0.0005
r46	10.9015	−3.5366	0.1870	0.0047	11.4115	−4.0124	0.3789	<.0001
r47	10.2872	−2.5997	0.2864	0.0003	9.9032	−2.4567	0.2532	0.0009
r56	6.3595	−0.7989	0.0038	0.7036	11.9325	−5.4508	0.2108	0.0029
r57	10.4835	−3.4048	0.1442	0.0143	9.5275	−2.8230	0.1007	0.0460
r67	8.8460	−2.8778	0.0773	0.0784	3.7809	1.2609	0.0121	0.4989

the tree crown sizes for stands in North Carolina. The tree crown sizes in Table 2b were used as validation. There were two outliers among the plots in Table 2b (plots 9 and 11), which we excluded in the validation. These two plots were regenerating hardwood stands with many small trees and a few large trees (see stem density in Table 2b). The large trees in the over story creates a rough canopy in the image, while the tree crown size measured on the ground was overwhelmed with small trees. Fig. 2a shows the comparison of measured CD and estimated CD based on an Ikonos image in North Carolina using the relationship derived from the Ikonos image from Ohio. The predicted CD is generally smaller than the measured CD ($R^2 = 0.75$, $P = 0.0$, RMSE = 0.79 m). Fig. 2b compares the measured CD with the CD estimated using the relationship derived from the QuickBird image in Ohio. Although they do not compare as well as in Fig. 2a, the accuracy ($R^2 = 0.52$, $P = 0.0$, RMSE = 0.79 m) is comparable with other approaches in the literature.

5. Discussion

This study found significant statistical evidence that the variance ratios of high spatial resolution optical images can be used to extract tree crown diameter for hardwoods stands though the accuracy is not as high as for coniferous stands. A previous study found that the approach worked well for coniferous stands but poorly for hardwood stands (Song, 2007). With more sampling plots and almost pure hardwood stands, this study has improved results compared with the previous study. We also found that the models developed can be generalized across sensors and sites. The statistical models developed with Ikonos and QuickBird images have almost identical slopes and intercepts even though the two images were collected at different years with very different image brightness values. Moreover, the models developed in Ohio can be directly applied to the image collected in North Carolina. The generalization capability could significantly broaden the sources of image and sampling data for mapping forest canopy structure.

5.1. Error analysis

The key to the success of extracting canopy structure from remote sensing is accuracy. Multiple factors in this study may influence the accuracy of tree crown size extracted in this study. These factors can be classified into two categories: exogenic and endogenic. Exogenic factors influence data quality. First, there is a time lag between ground data and image data. In Duke Forest, NC, the image was acquired on September 23, 2004, while the field data were collected in the summer of 2005. In Vinton Furnace Experimental Forest, ground data were collected in the summers of 2005 and 2007, while the images were collected in 2006 and 2007. The tree crown size in the image is different, though slightly, from the tree size sampled as a result of growth during the time lag. The difference may increase the RMSE between estimated tree crown size and tree size measured on ground. Planning a simultaneous collection of images and ground data is challenging as image acquisition depends on the weather conditions. Second, the field data were collected by two groups of people. Though both groups are working under the same protocol, there are still differences in data quality between the datasets collected in 2005 and 2007 as seen in Table 3. Third, topography and off-nadir viewing and illumination angles can make the apparent tree size in the image different from the real tree size. Although trees are always vertical regardless whether they grow on a slope or on a flat surface, topography and off-nadir illumination can change the amount of shadows in the image seen by the sensors (Schaaf et al., 1994). Off-nadir viewing changes the size of the projected tree crowns in the image. Although all the images were collected with viewing angle very close to nadir, the sun elevation angle for the North Carolina Ikonos image is quite different from those in Ohio.

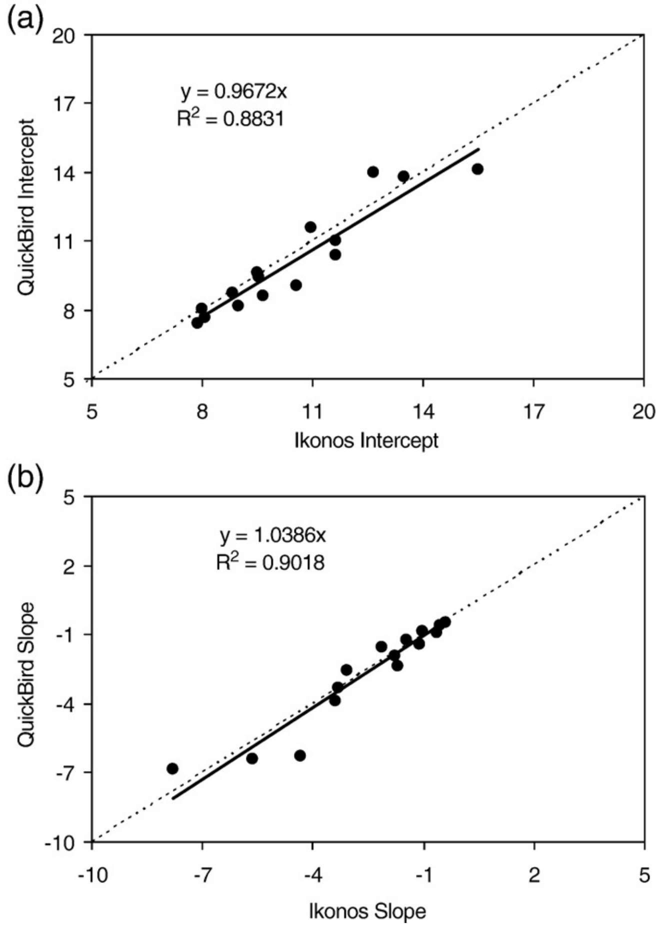

Fig. 2. The relationship between the slope and intercept in using the ratio of image variance at two spatial resolutions to derive CD from Ikonos and QuickBird image, respectively. The empirical model is $Y = a + bX$, where Y is CD and X is the ratio of image variance at two spatial resolutions. The empirical model is applied to Ikonos and QuickBird images, respectively, using the plots listed in Table 2a. (a): the slopes of the model using the Ikonos image vs. those using the QuickBird image; (b) the intercept of the model using the Ikonos vs. those using the QuickBird image.

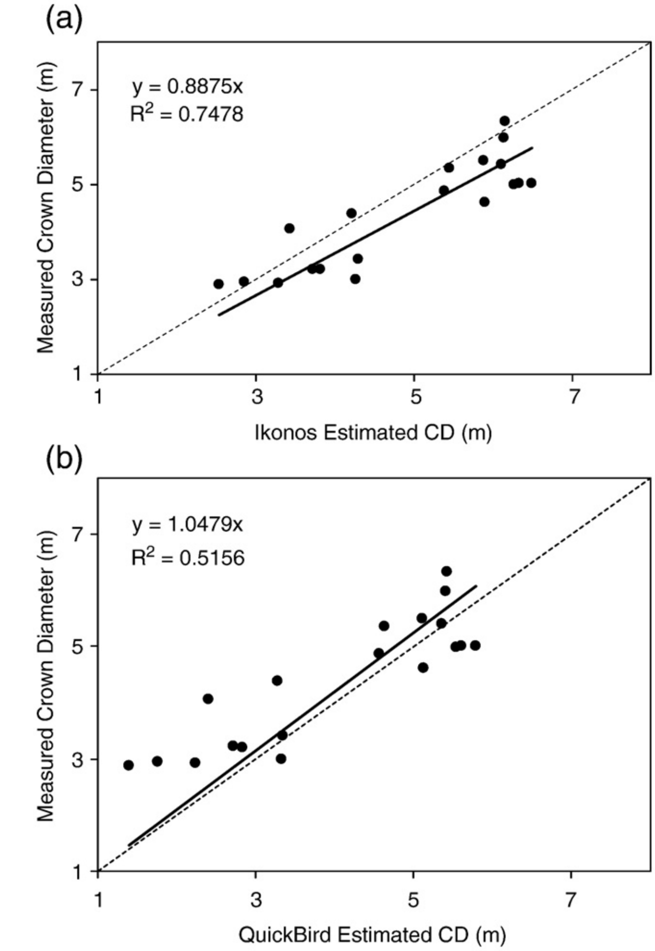

Fig. 3. Across-site application of models estimating CD using the ratio of image variances. (a) Comparison of measured CD in North Carolina with estimated CD using the model developed with the Ikonos image in Ohio and the Ikonos image in North Carolina. (b) The same as (a) except the QuickBird image in Ohio is used.

Endogenic factors relate to the fitness of model abstraction of the real world. The automatic approaches delineating tree crowns often assume a circular tree crown shape projected from above (Falkowski et al., 2006; Popescu et al., 2003). This study also assumes circular projected tree crown shape. We calculated the ellipticity of all the sampled tree crowns and estimated a stand ellipticity. The mean stand ellipticity is 1.25 ± 0.09 for the plots measured in Ohio in 2005, indicating tree crowns in general are not a perfect circle, but rather an ellipse with the major axis 25% longer than the minor axis. Deviation of tree crown shape from the assumption will influence the overlap function in Eq. (3), making the semivariogram anisotropic. However, as long as the sizes of the projected crowns do not change, the loss of overlap fraction in one direction will be made up by the gain of overlap fraction in another direction. The directional effect will disappear after the semivariogram reaches the sill. In this study, the dimension of the stand is much larger than the range of the image semivariogram, therefore, the shape of the crown will not have an effect on the image variance.

Fig. 3 shows that there is a slight overestimate of CD in Fig. 3a, and a slight underestimate in Fig. 3b. It is interesting to note that the RMSE values for both predictions are 0.79 m due to the across sensor generalization. The mean error for using relationship from Ikonos image is 0.50 m and −0.38 m from QuickBird. Wolter et al., (2009) reported that the RMSE for estimating tree crown size varies between 0.47 and 1.41 m in the literature, including both optical and Lidar imagery. Therefore, the errors in this study are comparable to those in other studies. The relative error in estimating tree crown size in this study is 18%. These results indicate that it is possible that the image variance ratio be used to estimate CD across sensors and sites.

5.2. Potential in estimating other canopy structure variables

Tree crown size is not only a critical canopy structural parameter for understanding forest ecosystem function (Song et al., 2009), but it is also significantly related to DBH, the major structural parameter that is often used to infer numerous other structural parameters (Gholz et al., 1979; Grier & Logan, 1977; Jenkins et al., 2004). Table 1 shows that there is a significant allometric relationships between CD and DBH on a species-specific basis. There is also a very strong statistical relationship between the average CD and DBH on the plot basis. Fig. 4 shows this relationship with the data in Table 2. Fig. 5 shows the potential of using variance ratios estimating the quadratic mean DBH at the stand scale. Though the statistical relationship is not as strong as for tree crown diameter, the relationship is statistically significant. It is interesting to note that the model parameters for the conifer dominated stands (Fig. 5a) and the hardwood dominated stands (Fig. 5b) are quite different. Therefore, the relationships are not generalizable because DBH is allometrically related to tree crown size which in turn depends on tree species. DBH is a primary forest

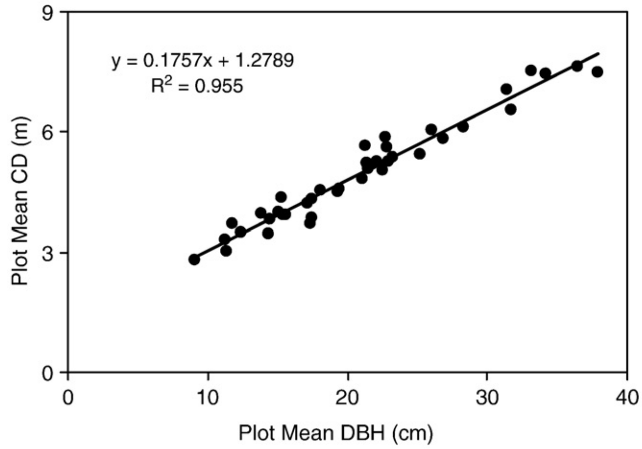

Fig. 4. The relationship between CD and DBH at the plot scale. The relationship is stronger than those on an individual-basis shown in Table 1.

inventory variable that can be used to estimate numerous other structural variables (Botkin et al., 1972; Gholz et al., 1979; Grier & Logan, 1977; Shugart & West, 1977; Urban, 1990). This indicates that the image variance ratio may be used to other canopy structural parameters (Song & Dickinson, 2008).

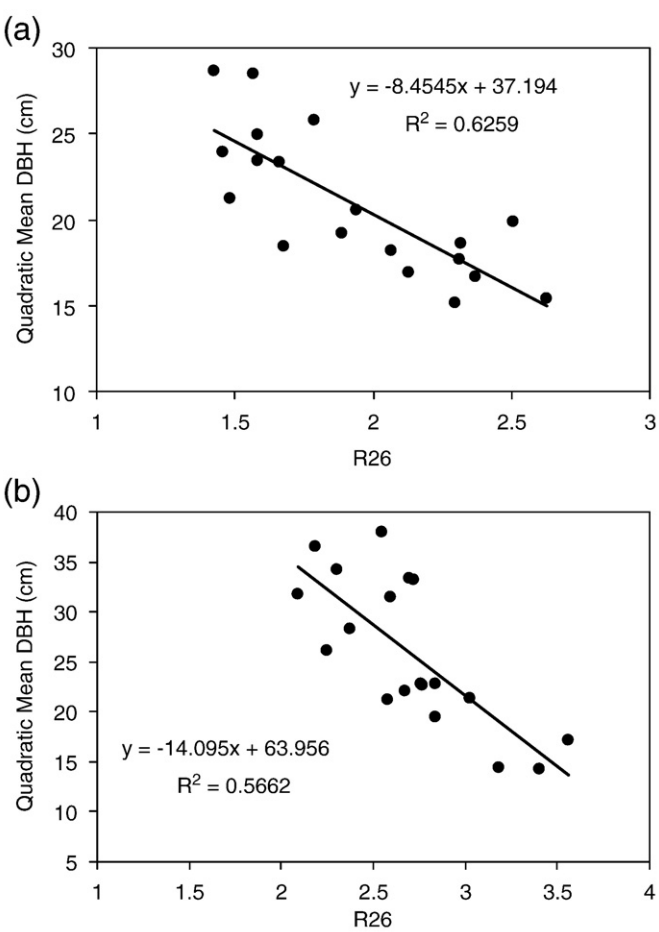

Fig. 5. The relationship between DBH and the ratio of image variance at 2×2 m to that at 6×6 m spatial resolution: (a) Conifer dominated sampling plots collected in 2005 and Ikonos image acquired 2004 in Duke Forest area in North Carolina Piedmont, and (b) Hardwood dominated sampling plots collected in 2005 and Ikonos image acquired in 2006 in REMA, Ohio.

6. Conclusions

This study investigated the potential of using the ratio of image variances at two spatial resolutions to estimate tree crown size for hardwood stands with Ikonos and QuickBird images. Although variance in tree crown size explained was not as high as in a previous study with stands dominated by conifers, the approach can provide estimates of average tree crown size for hardwood stands with accuracy comparable with other approaches in the literature. It is also possible that the model using the ratio of image variances at two spatial resolutions to predict CD can be generalized across sensors and sites. Both the slopes and intercepts for the empirical relationships developed from Ikonos and QuickBird images at the same place fall closely along the 1:1 line, particularly for models with relatively high R^2. We also found that models developed in Ohio can be applied directly to estimate tree crown size in North Carolina. Therefore, it is possible to take advantage of the existing images and forest inventory plot data to extract forest canopy structure at another place and time.

Acknowledgements

This study is partly supported by the USDA Forest Service Agenda 2020 program by NASA Grant NNX06AE28G. The authors wish to thank Ms. Andrea Nifong, Ms. Elizabeth Ward, and Mr. Bo Xiao for their assistance to the fieldwork in 2005.

References

Asner, G. P., Palace, M., Keller, M., Pereira, R., Silva, J. N. M., & Zweede, J. C. (2002). Estimating canopy structure in an Amazon Forest from laser range finder and IKONOS satellite observations. *Biotropica*, *34*(4), 483−492.

Botkin, D. B., Janak, J. F., & Wallis, J. R. (1972). Rationale, limitations, and assumptions of a northeastern forest growth simulator. *IBM Journal of Research and Development*, *16*, 101−116.

Brandtberg, T., & Walter, F. (1998). Automated delineation of individual tree crowns in high spatial resolution aerial images by multiple-scale analysis. *Machine Vision and Applications*, *11*, 64−73.

Brown, S., Pearson, T., Slaymaker, D., Ambagis, S., Moore, N., Novelo, D., et al. (2005). Creating a virtual tropical forest from three dimensional aerial imagery to estimate carbon stocks. *Ecological Applications*, *15*(3), 1083−1095.

Chen, D. X., & Coughenour, M. B. (1994). GEMTM — A general-model for energy and mass-transfer of land surfaces and its application at the FIFE sites. *Agricultural and Forest Meteorology*, *68*(3–4), 145−171.

Clark, D. B., Read, J. M., Clark, M. L., Cruz, A. M., Dotti, M. F., & Clark, D. A. (2004). Application of 1-M and 4-M resolution satellite data to ecological studies of tropical rain forests. *Ecological Applications*, *14*(1), 61−74.

Cohen, W. B., & Spies, T. A. (1992). Estimating structural attributes of Douglas-fir/western hemlock forest stands from Landsat and SPOT imagery. *Remote Sensing of Environment*, *41*, 1−17.

Culvenor, D. S. (2002). TIDA: An algorithm for the delineation of tree crowns in high spatial resolution remotely sensed imagery. *Computers and Geosciences*, *28*, 33−44.

Falkowski, M. J., Smith, A. M. S., Hudak, A. T., Gessler, P. E., Vierling, L. A., & Crookston, N. L. (2006). Automated estimation of individual conifer tree height and crown diameter via two-dimensional spatial wavelet analysis of Lidar data. *Canadian Journal of Remote Sensing*, *32*, 153−161.

Falkowski, M. J., Smith, A. M. S., Gessler, P. E., Hudak, A. T., Vierling, L. A., & Evans, J. S. (2008). The influence of conifer forest canopy cover on the accuracy of two individual tree measurement algorithms using Lidar data. *Canadian Journal of Remote Sensing*, *34*, S338−S350.

Franklin, J., & Strahler, A. H. (1988). Invertible canopy reflectance modeling of vegetation structure in semi-arid woodland. *IEEE Transactions on Geoscience and Remote Sensing*, *26*, 809−825.

Gholz, H. L., Grier, C. C., Campbell, A. G., & Brown, A. T. (1979). *Equations for estimating biomass and leaf area of plants in the Pacific Northwest.* : Forest Research Laboratory, School of Forestry, Oregon State University.

Grier, C. C., & Logan, R. S. (1977). Old-growth *Pseudotsuga menziesii* of a western Oregon watershed: Biomass distribution and production budgets. *Ecological Monographs*, *47*, 373−400.

Heurich, M. (2008). Automatic recognition and measurement of single trees based on data from airborne laser scanning over the richly structured natural forests of the Bavarian Forest National Park. *Forest Ecology and Management*, *255*, 2,416−2,433.

Jenkins, J. C., Chojnacky, D. C., Heath, L. S., & Birdsey, R. A. (2004). Comprehensive database of diameter-based biomass regressions for North America tree species. *USDA Forest Service, General Technical Report NE-319*.

Jupp, D. L B. 1999. INVDISK — Inversion of disk model "images" using mean, variance & variogram data. unpublished work through personal communication.

Jupp, D. L. B., Strahler, A. H., & Woodcock, C. E. (1988). Auto-correlation and regularization in digital images: 1. Basic theory. *IEEE Transactions on Geoscience and Remote Sensing*, *26*(4), 463−473.

Leckie, D. G., Gougeon, F. A., Walsworth, N., & Pardine, D. (2003). Stand delineation and composition estimation using semi-automated individual tree crown analysis. *Remote Sensing of Environment*, *85*, 355−369.

Lee, A. C., & Lucas, R. M. (2007). A LiDAR-derived canopy density model for tree item and crown mapping in Australian forests. *Remote Sensing of Environment*, *111*, 493−518.

Ni, W., Li, X., Woodcock, C. E., Boujean, J., & Davis, R. E. (1997). Transmission of solar radiation in boreal conifer forests: Measurements and models. *Journal of Geophysical Research*, *102*(D24), 29,555−29,566.

Palace, M., Keller, M., Asner, G. P., Hagen, S., & Braswell, B. (2008). Amazon forest structure from IKONOS satellite data and the automated characterization of forest canopy properties. *Biotropica*, *40*(2), 141−150.

Persson, A., Holmgren, J., & Soderman, U. (2002). Detecting and measuring individual trees using an airborne laser scanner. *Photogrammetric Engineering and Remote Sensing*, *68*, 925−932.

Pollock, R. J. (1996). A model-based approach to automatically locating individual tree crowns in high-resolution images of forest canopies. PhD Dissertation, Department of Computer Science, University of British Columbia, Vancouver, Canada.

Popescu, S. C., & Wynne, R. H. (2004). Seeing the trees in the forest: Using Lidar and multispectral data fusion with local filtering and variable window size for estimating tree height. *Photogrammetric Engineering and Remote Sensing*, *70*, 589−604.

Popescu, S. C., Wynne, R. H., & Nelson, R. E. (2003). Measuring individual tree crown diameter with Lidar and assessing its influence on estimating forest volume and biomass. *Canadian Journal of Remote Sensing*, *29*, 564−577.

Pouliot, D. A., King, D. J., Bell, F. W., & Pitt, D. G. (2002). Automated tree crown detection and delineation in high-resolution digital camera imagery of coniferous forest regeneration. *Remote Sensing of Environment*, *82*, 322−334.

Schaaf, C. B., Li, X., & Strahler, A. H. (1994). Topographic effects on bidirectional and hemispherical reflectances calculated with a geometric-optical canopy model. *IEEE Transactions on Geoscience and Remote Sensing*, *32*(6), 1186−1193.

Shugart, H. H., & West, D. C. (1977). Development of an Appalachian deciduous forest succession model and its application to assessment of the impact of the chestnut blight. *Journal of Environmental Management*, *5*, 161−179.

Song, C. (2007). Estimating tree crown size with spatial information of high resolution optical remotely sensed imagery. *International Journal of Remote Sensing*, *28*(15), 3305−3322.

Song, C., & Band, L. E. (2004). MVP: A model to simulate the spatial patterns of photosynthetically active radiation under discrete forest canopies. *Canadian Journal of Forest Research*, *34*, 1192−1203.

Song, C., & Dickinson, M. B. (2008). Extracting forest canopy structure from spatial information of high resolution optical imagery: Tree crown size versus leaf area index. *International Journal of Remote Sensing*, *29*(19), 5605−5622.

Song, C., & Woodcock, C. E. (2003). Estimating tree crown size from multiresolution remotely sensed imagery. *Photogrammetric Engineering and Remote Sensing*, *69*(11), 1263−1270.

Song, C., Katul, G., Oren, R., Band, L. E., Tague, C. L., Stoy, P. C., et al. (2009). Energy, water and carbon fluxes in a loblolly pine stand: Results from uniform and gappy canopy models with comparisons to eddy flux data. *Journal of Geophysical Research-Biogeosciences*, *114*, G04021. doi:10.1029/2009JG000951

Strahler, A. H., Woodcock, C. E., & Smith, J. A. (1986). On the nature of models in remote sensing. *Remote Sensing of Environment*, *20*, 121−139.

Urban, D. L. (1990). *A versatile model to simulate forest pattern: A user's guide to ZELIG, version 1.0.* Charlottesville, VA: University of Virginia.

Wang, L., Sousa, W. P., Gong, P., & Biging, G. S. (2004). Comparison of IKONOS and QuickBird images for mapping mangrove species on the Caribbean coast of Panama. *Remote Sensing of Environment*, *91*(3–4), 432−440.

Wolter, P. T., Townsend, P. A., & Sturtevant, B. R. (2009). Estimation of forest structural parameters using 5 and 10 meter SPOT-5 satellite data. *Remote Sensing of Environment*, *113*(9), 2019−2036.

Woodcock, C. E., Strahler, A. H., & Jupp, D. L. B. (1988). The use of variograms in remote sensing: I. *Scene models and simulated images, Remote Sensing of Environment*, *25*, 323−348.

Woodcock, C. E., Strahler, A. H., & Jupp, D. L. B. (1988). The use of variograms in remote sensing: II. Real digital images. *Remote Sensing of Environment*, *25*, 349−379.

Woodcock, C. E., Collins, J. B., Gopal, S., Jakabhazy, V. D., Li, X., Macomber, S. A., et al. (1994). Mapping forest vegetation using Landsat TM imagery and a canopy reflectance model. *Remote Sensing of Environment*, *50*, 240−254.

Woodcock, C. E., Collins, J. B., Jakabhazy, V. D., Li, X., Macomber, S. A., & Wu, Y. (1997). Inversion of the Li-Strahler canopy reflectance model for mapping forest structure. *IEEE Transactions on Geoscience and Remote Sensing*, *35*, 405−414.

Wu, Y., & Strahler, A. H. (1993). Remote estimation of crown size, stand density and foliage biomass on the Oregon transect. *Ecological Application*, *4*, 299−312.

Wulder, M., Niemann, K. O., & Goodenough, D. (2000). Local maximum filtering for the extraction of tree locations and basal area from high spatial resolution imagery. *Remote Sensing of Environment*, *73*(1), 103−114.

Wulder, M. A., White, J. C., Niemann, K. O., & Nelson, T. (2004). Comparison of airborne and satellite high spatial resolution data for the identification of individual trees with local maxima filtering. *International Journal of Remote Sensing*, *25*(11), 2225−2232.